

# THE CLUSTER MAGNETIC FIELD INVESTIGATION

A. BALOGH, M. W. DUNLOP, S. W. H. COWLEY, D. J. SOUTHWOOD and  
J. G. THOMLINSON

*The Blackett Laboratory, Imperial College, London, U.K.*

K. H. GLASSMEIER, G. MUSMANN, H. LÜHR and S. BUCHERT  
*Institut für Geophysik und Meteorologie, Technische Universität Braunschweig, Germany*

M. H. ACUÑA, D. H. FAIRFIELD and J. A. SLAVIN  
*Goddard Space Flight Center, Greenbelt, MD., U.S.A.*

W. RIEDLER and K. SCHWINGENSCHUH  
*Institut für Weltraumforschung, Graz, Austria*

M. G. KIVELSON  
*Institute for Geophysics and Planetary Physics, University of California, Los Angeles, CA., U.S.A.*

## THE CLUSTER MAGNETOMETER TEAM

**Abstract.** The Cluster mission provides a new opportunity to study plasma processes and structures in the near-Earth plasma environment. Four-point measurements of the magnetic field will enable the analysis of the three dimensional structure and dynamics of a range of phenomena which shape the macroscopic properties of the magnetosphere. Difference measurements of the magnetic field data will be combined to derive a range of parameters, such as the current density vector, wave vectors, and discontinuity normals and curvatures, using classical time series analysis techniques iteratively with physical models and simulation of the phenomena encountered along the Cluster orbit. The control and understanding of error sources which affect the four-point measurements are integral parts of the analysis techniques to be used. The flight instrumentation consists of two, tri-axial fluxgate magnetometers and an on-board data-processing unit on each spacecraft, built using a highly fault-tolerant architecture. High vector sample rates (up to 67 vectors  $\text{s}^{-1}$ ) at high resolution (up to 8 pT) are combined with on-board event detection software and a burst memory to capture the signature of a range of dynamic phenomena. Data-processing plans are designed to ensure rapid dissemination of magnetic-field data to underpin the collaborative analysis of magnetospheric phenomena encountered by Cluster.

## 1. Introduction: Overview of Objectives

The four-spacecraft Cluster mission (Escoubet *et al.*; Credland *et al.*, this issue) will provide the first opportunity to determine the three-dimensional, time-dependent characteristics of small-scale processes and structures in the near-Earth space plasma, both in the magnetosphere and in the nearby interplanetary medium. Small-scale phenomena, such as localised, transient magnetic reconnection (flux transfer events) or turbulent diffusion, which operate at the boundaries between plasmas of different origin, are largely responsible for determining the nature and geometry of the interactions. The objectives of the Cluster mission and of the magnetic-field

investigation are the study of phenomena on spatial scales corresponding to the proposed separation distances of the four spacecraft and their interpretation in terms of the role they play on a more global scale to shape the properties of different regions of the magnetosphere and the upstream solar wind.

Cluster will sample most of the key regions of the magnetosphere: the dayside magnetospheric boundary, both at mid-latitudes and in the cusp, where processes associated with magnetic reconnection and turbulence are believed to occur; the near-Earth magnetospheric tail on the nightside which undergoes frequent large-scale magnetic reconfigurations during substorms; and the upstream solar wind, bow shock and magnetosheath. The anisotropy which is inherent in all magnetised plasma processes, introduced by the magnetic field, makes the accurate determination of the magnetic field at high time resolution a critical contribution to the probing of small-scale structures and dynamics encountered in these regions.

The Cluster mission was conceived to overcome some of the inherent limitations and difficulties in interpreting previous magnetospheric observations, which were made overwhelmingly by a single spacecraft. The range of phenomena in the magnetosphere and its boundaries that can be uniquely addressed by multi-point magnetic field measurements is considerable. The following examples are used to illustrate, rather than exhaustively to describe, the potential advantages of the four-spacecraft observations.

The current understanding of the structure and dynamics of the main boundaries on the sunward side of the magnetosphere, the bow shock and the magnetopause, is based to a large extent on observations of single crossings and numerical simulations. However, as shown by dual spacecraft observations, these boundaries have complex, evolving structures and are non-stationary on several time- and length scales (see, for example, the reviews of upstream waves, bow shock and magnetopause observations by Russell (1989), Thomsen (1989), and Elphic (1989), respectively). Four-point magnetic-field observations are expected to provide information on the immediate neighbourhood of the boundaries which will clarify the phenomenology of boundary-associated phenomena simultaneously at the four locations. A particularly interesting objective of Cluster on this topic is the exploration of processes occurring at quasi-parallel bow shock geometries, where the generally accepted shock re-formation occurs (Burgess, 1989; Scholer and Burgess, 1992), as has been shown by increasingly sophisticated simulations (e.g., Scholer *et al.*, 1993; Giacalone *et al.*, 1994). Boundary crossing phenomena include complex wave fields that are an integral part of the MHD processes that form the wider environment of the boundaries; inherent non-stationarity prevents the resolution of these wave fields by single- or even two-point measurements. During a two-year mission, Cluster will cross the dayside bow shock and magnetopause several hundred times. This will allow the observation of both boundaries under a range of conditions which will provide the basis for a separation of different phenomena and causal processes. The magnetometers on Cluster, with their high time resolution

and their event-driven Microstructure Analyser (see Section 3), will generate the necessary data sets to determine the context and processes at these boundaries.

Other specific phenomena for four-point analysis to which the observations of the magnetic field on Cluster will contribute include dayside magnetic reconnection and the nature of flux transfer events in particular; the role of the Kelvin–Helmholtz instability in magnetopause processes; impulsive events, possibly driven by discontinuities in the solar wind; and, as a prime objective of Cluster, the nature, structure and dynamics of the outer cusp (as summarised for example by Paschmann, 1995; Scholer, 1995).

In the magnetospheric tail, Cluster observations will target both phenomena at small scales, such as the structure and time evolution of current sheets associated with the growth phase of substorms and, on larger scales, to establish the magnetic topology of the different regions in the tail and their dynamics. The role, in particular, of a range of current structures and their magnetic signatures, all on scales which require high time resolution magnetic measurements, simultaneously at several locations, will contribute to resolving the time evolution of the magnetospheric tail prior to and during substorms (as summarised for example by Cowley, 1995; Roux and Sauvaud, 1995).

A significant subset of the objectives of the magnetic field investigation has close connections with the wider field of solar-terrestrial relations. In this context, collaboration with simultaneous ground-based observations will play a key role in relating magnetospheric responses with signatures observed by remote-sensing, ground-based instruments and facilities, such as magnetometer chains and ionospheric radars (Oppennoorth *et al.*, this issue).

The analysis of four-point magnetic field measurements presents formidable conceptual and technical challenges. In Section 2, we outline the main strands of scientific data analysis techniques which have been developed or considered for the Cluster magnetic-field investigation and comment on their expected applicability. Some of these techniques, together with details of their applications and the complexities of the expected results are summarised in this paper. The evolution of the Cluster orbit, the configuration of the tetrahedron and the separation distances are discussed briefly, in the light of the importance of the orientation and shape of the tetrahedron along the orbit with respect to the magnetic field in the different regions of the magnetosphere.

While magnetometers, in particular of the fluxgate type, have been the mainstay of magnetospheric missions, the design of the Cluster magnetometers presents specificities which are described in Section 3. More details of the instrument functions can be found in Balogh *et al.* (1993). The intercalibration of the magnetometers on the four spacecraft is a major requirement, as the combined analysis of the data is largely based on the measurement of differences between spacecraft. Error analysis, ground calibration and plans for in-flight calibration procedures have therefore played a greater than usual role in the pre-launch development of the instrument; these are summarised in Section 4.

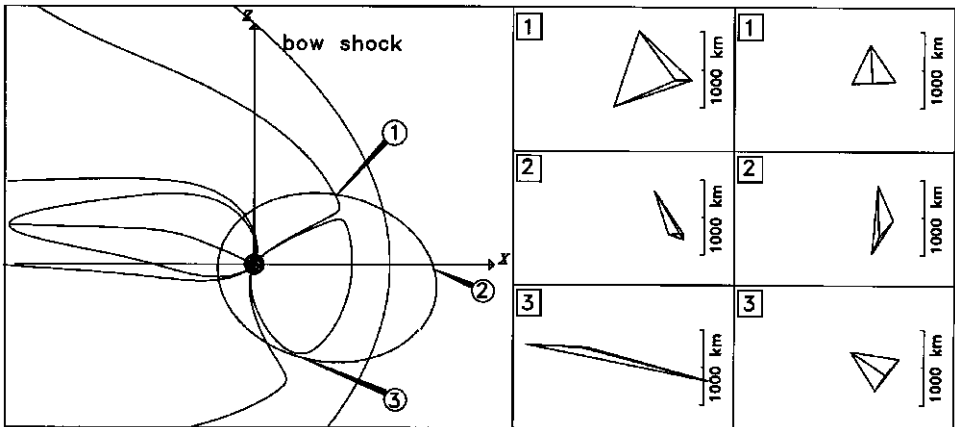


Figure 1. Model orbit of Cluster in the noon-midnight meridian, with representative shapes of the Cluster tetrahedron corresponding to different separation strategies.

The orbit selected for Cluster is polar, with a perigee of  $4 R_E$  and an apogee of  $19.6 R_E$ . The shape of the four-spacecraft Cluster configuration is basically a tetrahedron which, once set up at a particular point, evolves around the orbit in a deterministic way (for example, Dunlop, 1990). The orbital evolution of the tetrahedral shape, its orientation and its degree of deformation with respect to both the main local anisotropies and the reference regular tetrahedron in the different regions of the magnetosphere, as well as the separation distances, all play a key role in constraining the applicable analysis techniques. While some of the parameters of the orbit and of the configuration are relatively free and will be tuned during the mission, others are more constrained by both operational and dynamic considerations.

For the purpose of illustrating the context of the measurements, Figure 1 represents one of the model orbits of Cluster, with the shape of the tetrahedron magnified at three locations. The orbit represents the epoch when the apogee of the spacecraft is on the sunward side of the magnetosphere. The two sets of tetrahedra correspond to two possible constellation strategies. The first is the baseline mission (although the exact details are dependent on launch date), with a regular tetrahedron set up at the location of the northern cusp. The second constellation strategy was developed by recognising inherent flexibilities in orienting the tetrahedron which allow, as a secondary constraint, the setting up of a regular tetrahedron at a second location (in this case, at the southern cusp) along the orbit. The deformation of the constellation at the location of the southern cusp in the first case illustrates well the evolution of the tetrahedron; the fact that both strategies are possible (and a significant range in between) illustrates the complexity involved in the planning of the different orbit strategies. Other significant and unforeseeable complications arise from the dynamic reactions of the magnetosphere to changing solar wind and

Table I  
Cluster magnetic field investigation (FGM) investigator team

A. Balogh (PI)	The Blackett Laboratory, Imperial College, London, U.K. D.J. Southwood
S.W.H. Cowley	Dept. of Physics and Astronomy, University of Leicester,
Leicester, U.K.	
K.-H. Glassmeier	Institut für Geophysik und Meteorologie,
H. Lühr	Technische Universität Braunschweig, Germany
G. Musmann	
M. H. Acuña	NASA/GSFC, Greenbelt, MD., U.S.A.
D. H. Fairfield	
J. A. Slavin	
W. Riedler	Institut für Weltraumforschung, Graz, Austria
K. Schwingenshuh	
F. M. Neubauer	Institut für Geophysik und Meteorologie, Universität zu Köln,
	Germany
M. G. Kivelson	Institute for Geophysics and Planetary Physics,
	UCLA, Los Angeles, CA., U.S.A.
M. Tatralay	RMKI/KFKI, Budapest, Hungary
R. C. Elphic	Los Alamos National Laboratory, NM, U.S.A.
F. Primdahl	Dansk Rumforskninginstitut, Lyngby, Denmark
A. Roux	CETP/USQV, Velizy, France
B. T. Tsurutani	Jet Propulsion Laboratory, Pasadena, CA, U.S.A.

interplanetary magnetic-field conditions; the magnetosphere illustrated is based on the Tsyganenko model, assuming moderately disturbed conditions. An early, but thorough discussion of the effects of the potential range of orbit and constellation parameters on magnetic field measurements and analysis can be found in Dunlop (1990).

The Cluster magnetic-field investigation is directly supported by a large scientific team, representing eleven institutions in seven countries. The investigator team is listed in Table I. Extensive plans for post-launch operations, data processing and exploitation have been drawn up; these are summarised in Section 5. The coordination of the data dissemination, through the Cluster Science Data System in particular will enable the establishment of early initiation of scientific cooperation between the magnetic field investigators, the Cluster community, and the wider interested science community.

## 2. Four-spacecraft Data Analysis Techniques

The most important attribute of the mission and of the magnetic-field investigation is the possibility that is provided to compare observations that are relatively closely spaced compared to the principal dimensions of the magnetosphere. It is anticipated that many of the processes on the scales to be sampled by Cluster are in fact those which shape the larger-scale structure and properties of the system. While much is known in terms of such larger-scale processes and structures, the small scale is often assumed rather than understood; in this sense, Cluster is an exploratory mission. The full phenomenology of small-scale processes is likely to be discovered during the mission. This necessitates the preparation of the data analysis of the forthcoming magnetic-field observations in terms of tools that recognise basic physical processes and structures. However, the likely complexity of phenomena on these scales, both temporally and spatially, implies the need for a flexible methodology to discern the underlying component processes. Therefore a dual approach, based on both the underlying physics and judicious modelling of more complex superpositions of temporal and spatial dependences, is required for data analysis.

In general terms, the analysis and interpretation of the Cluster magnetic-field data has to proceed by successively iterating assumed models, based on expectations derived from knowledge or assumptions about magnetospheric structures and processes, and their goodness of fit to the data. This general analysis procedure is illustrated in Figure 2. Despite the apparently self-evident generality of this procedure, a detailed analysis of the methodology in these terms is essential to identify the specific problems and the applicability of any data-analysis technique to the case of the Cluster magnetic-field data. Several studies based on this general methodology, applied to the expected Cluster magnetic-field data, have explored specific aspects of the problem of interpreting observed signatures in terms of a known input model.

Given that the Cluster magnetic-field data set consists of the vector measurements of the magnetic field at the location of the four Cluster spacecraft, combined with the location and time of the measurements, three different data analysis techniques have been considered. These are the curlometer, the wave telescope and the discontinuity analyser, as summarised in Table II. As shown in the Table, the main distinguishing feature of the three techniques is their applicability relative to the scale sizes of the basic phenomena to be analysed. This interaction between scale size and spacecraft separation is one of the main characteristics of the expected magnetic-field observations.

The next level of complexity in the magnetometer data analysis arises as a result of fundamental anisotropies in the magnetosphere. While it is assumed that the best basic configuration of the Cluster tetrahedron is a regular one, the spacecraft constellation naturally evolves through the orbit. This leads to the need to consider the dominant orientation (e.g., the elongation) of the four-spacecraft configuration with respect to the natural anisotropies in the different magnetospheric regions

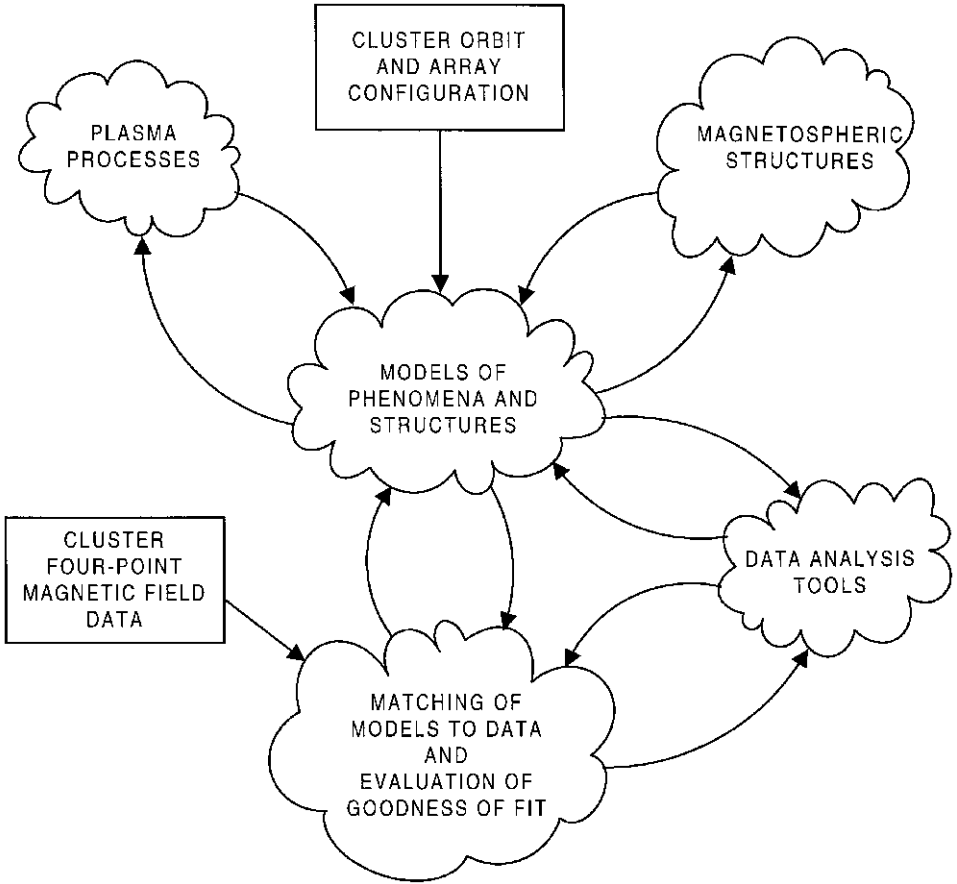


Figure 2. Conceptual methodology for the analysis of four-point magnetic field data from Cluster, representing the need for multiple iteration between data analysis techniques and physical modelling of magnetospheric phenomena.

Table II

Relative scales	Analysis technique	Representative expression
$L > \mathbf{R}_{ij}$	Curlometer	$\mu_0 \mathbf{J} \cdot (\Delta \mathbf{R}_i \times \Delta \mathbf{R}_j) = \Delta \mathbf{B}_i \cdot \Delta \mathbf{R}_j - \Delta \mathbf{B}_j \cdot \Delta \mathbf{R}_i$ $\langle \text{div } \mathbf{B} \rangle_{\text{average}} = 0$
$L \approx \mathbf{R}_{ij}$	Wave telescope	$\phi_i = \mathbf{k} \cdot \Delta \mathbf{R}_i - \omega \Delta t_{ij}$ $\mathbf{k} = \mathbf{k}_0 + \mathbf{G}$
$L < \mathbf{R}_{ij}$	Discontinuity analyser	$\langle n \rangle, n_j, v_{  }, a_{  }$

encountered by Cluster. The orientation and scale length of the tetrahedron with respect to the background magnetic field, the background flow and the normals to discontinuity surfaces (bow shock, magnetopause) strongly condition the expected differential magnetic signatures, and therefore the most appropriate analysis tools to be used for the identification of specific small-scale properties of the plasma phenomena. An overview of the relationship between phenomena expected in and near the magnetosheath, their anisotropic properties and the applicability of data-analysis tools has been given in Dunlop *et al.* (1993). In the magnetosheath, the interplay between the orientation of the Cluster tetrahedron with respect to the dominant flow and field directions on the one hand, and the applicability of analysis tools on the other, results in the sampling of extended structures along the background field, short scales transverse to the field and intermediate scales roughly along the direction of the flow component transverse to the magnetic field. Other regions of the magnetosphere will present other combinations between the measurement anisotropies (due to the shape of the tetrahedron and the use of different data analysis methods) and the preferred orientation and scale sizes of static and dynamic magnetospheric phenomena.

The combination of vector differences between simultaneous measurements at the four locations, using Maxwell's equations, can be interpreted in terms of the average current density of the plasma. This technique (the curlometer) yields, assuming stationarity, a measure of the components of the current density vector. However, simple modelling of curlometer measurements in a model magnetosphere have shown (Dunlop *et al.*, 1990) that field gradients on the scale of, or shorter than the Cluster separation can bias the estimate of the current density vector, indicated by the implied non-zero divergence of the vector differences. It is important to recognise that natural gradients in a static model magnetosphere already introduce such distortions in the estimates based on four-spacecraft data; in other words, the technique is sensitive to the global current systems which shape the magnetosphere. Several model studies (Dunlop *et al.*, 1990; Robert and Roux, 1993; Dunlop and Balogh, 1993; Robert *et al.*, 1995) along the Cluster orbit have explored the sensitivity of the current density estimates based on difference measurements to the shape of the Cluster tetrahedron.

Dynamic effects, on both large- and small-scales, are additional sources of current which affect the curlometer output. Nevertheless, a routine measure of the current density, implied by the difference measurements of the magnetic field, can detect the presence and direction of local current systems.

The variability of the magnetic field on scales comparable to the spacecraft separation vectors can be examined in terms of 'waves'. The 'wave telescope' method of data analysis has already been extensively investigated in connection with Cluster (for example Neubauer and Glassmeier, 1990; Neubauer *et al.*, 1990; Motschmann *et al.*, 1995a, b). The complexity of the possible wave fields and the task to describe them in terms of self-consistent sets of quantitative parameters require the use, not just of advanced signal analysis techniques, but also a range of

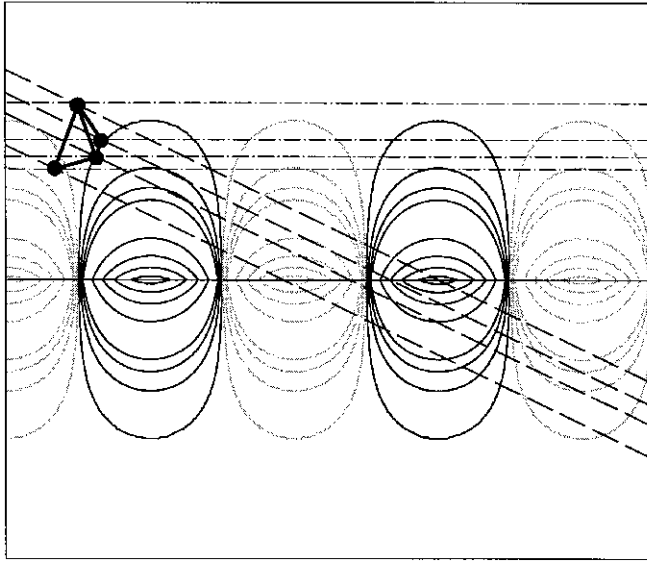


physical assumptions (Pinçon and Lefeuvre, 1991, Motschmann and Glassmeier, 1995, Motschmann *et al.*, 1995b, Pinçon, 1995). Temporal and spatial stationarity can be assumed only as a first approximation; the small-scale dynamics of magnetospheric processes will invariably lead to the need to consider, almost on a case-by-case basis, an iterative approach of data analysis as outlined above.

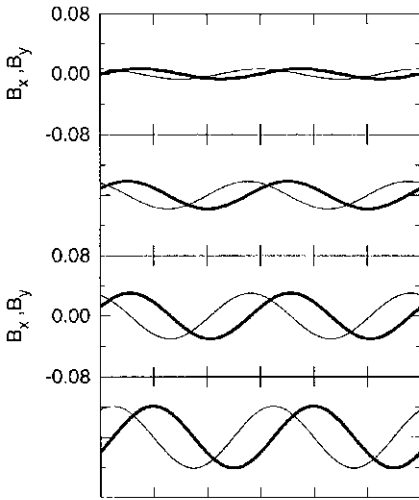
The third basic tool to be used for the analysis of the magnetic-field data from the four Cluster spacecraft is the discontinuity analyser. Recognising that boundaries between plasma regimes are almost always in motion, a simple fitting of the times of boundary crossings detected at the four locations is unlikely to be sufficient. The minimum-variance technique (Sonnerup and Cahill, 1967), originally developed for the study of boundary crossings by single spacecraft, has been extensively developed and applied to the determination of boundary normals in space plasmas. Application of minimum-variance analysis to the Cluster magnetic field data has required a re-evaluation of this technique (Dunlop *et al.*, 1995a) to explore its limitations and to delineate the conditions for its use. Other techniques also need to be investigated (Chapman and Dunlop, 1993; Watkins *et al.*, 1995). The starting point may be the application of the technique to single-spacecraft data, followed by a comparison of the properties (normals and velocities) derived at the four points. An ideal set would provide at most small differences between the normal directions, thus satisfying the condition for (near) planarity of the boundary. It is expected that an important class of boundary crossings will satisfy the near-planarity condition, as well that of near-stationarity (i.e., when the boundary crossing is fast compared to the evolution of the Cluster tetrahedron).

However, if the normals determined at the four locations are significantly different, more complex assumptions need to be built into the data analysis (Dunlop *et al.*, 1995b). Some important non-planar structures expected are flux transfer events and field-line resonance structures. A hierarchical data analysis approach, iteratively feeding back data on the event parameters to improve a modelled boundary structure, is needed to resolve the overdetermined, but ambiguous four-spacecraft data. Complex boundaries where time stationarity breaks down significantly, such as quasi-parallel bow shock crossings, represent an important target for Cluster where extremes of temporal and spatial variability are expected (Giacalone *et al.*, 1994; Burgess, 1995). Even one-dimensional simulations of the shock reformation process which characterises the dynamics of the high Mach number, quasi-parallel bow shock illustrate well the challenge posed to Cluster to detect the spatial and temporal evolution of such shock waves.

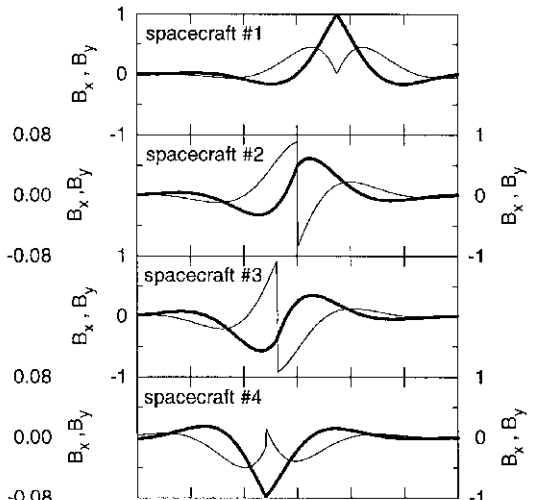
An illustration of Cluster magnetic field measurements through a simple non-planar two dimensional spatial structure is given in Figure 3. The magnetic field is defined by  $b_x = B_0 e^{-ikx} e^{-k|y|}$ ,  $b_y = ib_x$  for  $y < 0$  and  $b_y = -ib_x$  for  $y > 0$ , with  $b_z$  an arbitrary constant. Ignoring this last component, the structure is that of a stationary sinusoidal wave along the  $x$  direction, with wave normal  $k$ , but with an exponentially decaying magnitude on either side of the  $y = 0$  axis. Two fly-throughs were considered (Dunlop *et al.*, 1995b), one parallel to



(a)



(b)



(c)

Figure 3. (a) Model of surface wave of the magnetic field and two possible Cluster trajectories through it. (The contour plot of  $b_x$  is shown.) (b) and (c) Signatures of the surface wave in (a) for the two sample trajectories of Cluster in the magnetic-field data. (Thick and thin lines show the  $b_x$  and  $b_y$  components, respectively.)

the  $x$  axis, and one obliquely across the structure, as illustrated in Figure 3(a). The ‘measured’  $b_x$  and  $b_y$  components for the two trajectories are illustrated in Figures 3(b) and 3(c), respectively. For the trajectory along the  $x$  axis, the two components are in quadrature, with different amplitudes measured at the location of the four spacecraft. A variance analysis yields a minimum direction along the  $z$  axis, clearly in contradiction with the geometry of the model. However, the non-planar nature of the structure can be deduced from the two components. The oblique trajectory yields, in the  $b_x$  component, the apparent signature of a wave packet, with a propagation vector approximately along the fly-through trajectory. The behaviour of the  $b_y$  component, with abrupt phase changes at the crossing of the  $y = 0$  surface, indicates, however, the true nature of the field configuration. The conclusions to be drawn from this simple example is that the signature of the magnetic field configuration in the Cluster data set will depend heavily on the respective orientations and scale sizes of the Cluster tetrahedron and the actual field geometry.

### 3. Instrumentation

Each Cluster spacecraft carries an identical instrument to measure the magnetic field. Each instrument, in turn, consists of two triaxial fluxgate magnetometers and an on-board Data-Processing Unit (DPU). The block diagram of the instrument is shown in Figure 4. The mass of each of the triaxial fluxgate sensors is 290 g, with an additional 48 g for the thermal cover. The mass of the electronics box is 2060 g. The instrument power consumption in normal operations is 2460 mW.

The fluxgate magnetometers are similar to many previous instruments flown in Earth-orbit and on other, planetary and interplanetary missions. In order to minimise the magnetic background of the spacecraft, one of the magnetometer sensors (the outboard, or OB sensor) is located at the end of one of the two 5.2 m radial booms of the spacecraft, the other (the inboard, or IB sensor) at 1.5 m inboard from the end of the boom. In flight, either sensor can be designated as the Primary Sensor, for acquiring the main data stream of magnetic-field vectors. Selection of the sensors as Primary or Secondary is made by ground command; in the default configuration, the OB sensor is used as the Primary Sensor. Data are also acquired simultaneously from the other, Secondary Sensor, albeit at a lower rate.

The magnetometers have eight possible operating ranges; of these, five are used on the Cluster magnetometers, shown in Table III. These ranges were selected to provide good resolution in the solar wind (with expected field magnitudes between 3 and 30 nT), and up to the highest field values expected in the magnetosphere along the Cluster orbit (up to about 1000 nT). The highest range (65 500 nT) is used only to facilitate ground testing. Range selection can be automatic (controlled by the instrument DPU) or commanded from the ground. When in the automatic mode, a range selection algorithm running in the DPU continuously monitors each

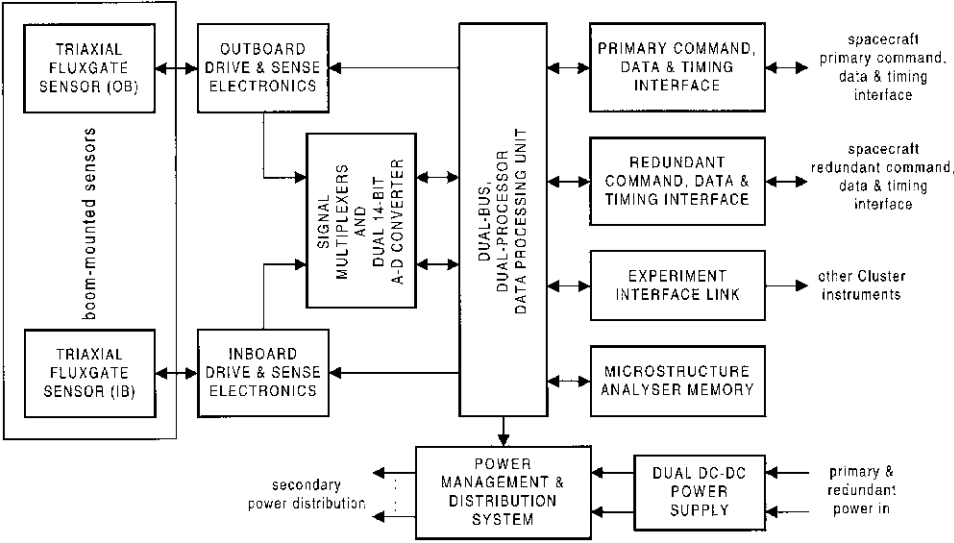


Figure 4. Block diagram of the Cluster magnetometer (FGM). The instrument has a high level of redundancy and fault tolerance.

Table III

Range (nT)	Digital resolution (nT)
−64 to +63.992	$7.813 \times 10^{-3}$
−265 to +255.97	$3.125 \times 10^{-2}$
−1024 to +1023.9	0.125
−4096 to +4095.5	0.5
−65536 to +65528	8

component of the measured field vector. If any component exceeds a fraction (set at 90%) of the range, an up-range command is generated and transmitted to the magnetometer. If all three components are smaller than 10% of the range for more than a complete spin period (in fact for more than the telemetry frame period of 5.15222 s), an automatic down-range command is generated to the magnetometer.

The instrument uses two 16-bit Analogue-to-Digital Converters (ADC), normally in cold redundancy. The most significant 14 bits of the converted field-component values are used for generating the output of the instrument. The digital resolution, corresponding to the five ranges of the magnetometers, is shown in Table III.

The DPU of the instrument contains two, redundant, Central Processing Units (CPU), based on the Low-Power Processor System developed by British Aerospace, using the MAS281 microprocessor, implementing the MIL-STD-1750A instruction set. The two CPUs are linked to each other and to other functions within the DPU

by a dual, redundant, data and address bus. Two, redundant spacecraft interface units are used to receive telecommands and to transmit data to the telemetry, via the two (primary and redundant) spacecraft command and telemetry interfaces. An internal power management system, controlled by ground commands, allows the selective switching of functional units within the DPU. The power switches can also automatically switch off functions in the DPU when an excessive current drain is detected. The instrument is powered by two, redundant, power converter units, which receive power independently from the spacecraft. The overall design of the instrument has a highly failure-tolerant architecture.

The data-acquisition process is controlled by the DPU. The three components of the magnetic-field vector measured by the Primary Sensor are sampled at a constant rate of 201.75 Hz, independently of the finally transmitted vector rate. Data acquired at this rate are digitally filtered to match the transmitted rate, according to the operating modes of the instrument and the telemetry data rate allocated to it.

The spacecraft telemetry operates in different modes, corresponding to different data acquisition and transmission rates for the different instruments. The magnetometer has been allocated four telemetry data rates, corresponding to the Nominal Mode (at 1211.13 bits  $s^{-1}$ ), Burst Mode 1 (3465.69 bits  $s^{-1}$ ), Burst Mode 2 (1347.77 bits  $s^{-1}$ ) and Burst Mode 3 (5583.61 bits  $s^{-1}$ ). The spacecraft telemetry is based on a packetised protocol, with a constant frame length of 5.15222 s, independent of telemetry rate. The vector data rates from the magnetometer associated with the different telemetry modes of the spacecraft are shown in Table IV. In the Nominal and Burst Mode 2 telemetry modes, the instrument uses three, commandable vector transmission rates (FGM Telemetry Options A, B, and C), distinguished by different rates for the Primary and Secondary Sensors, and the data rate read out from the Microstructure Analyser memory. In Burst Mode 1, no data are read out from the Microstructure Analyser memory. In Burst Mode 3, scheduled collectively for all the instruments with burst memory capabilities, data are dumped fast from the Microstructure Analyser memory. The magnetometer DPU uses Gaussian-windowed digital filtering to reduce the stream of primary vector samples to match the bandwidth of the telemetry. Figure 5 shows (in the upper panel) the (unnormalised) weights associated with the transmitted vector data rates and (in the lower panel) the weighting of successive transmitted vector samples at the 15.5 vectors  $s^{-1}$  rate.

The instrument incorporates a Microstructure Analyser (MSA) which consists of a burst memory capable of storing about 32 000 magnetic field vectors, and the associated event recognition software in the DPU. The objective of the MSA is to record events of short duration, at acquisition rates not available at normal or burst telemetry rates, when the magnetic signature of the event satisfies programmable preset criteria. Data recorded in the MSA are read out in the telemetry either in a background mode, in parallel with the normal data acquisition, or in a short burst, in Burst Mode 3 of the spacecraft telemetry. Considerable flexibility has been built

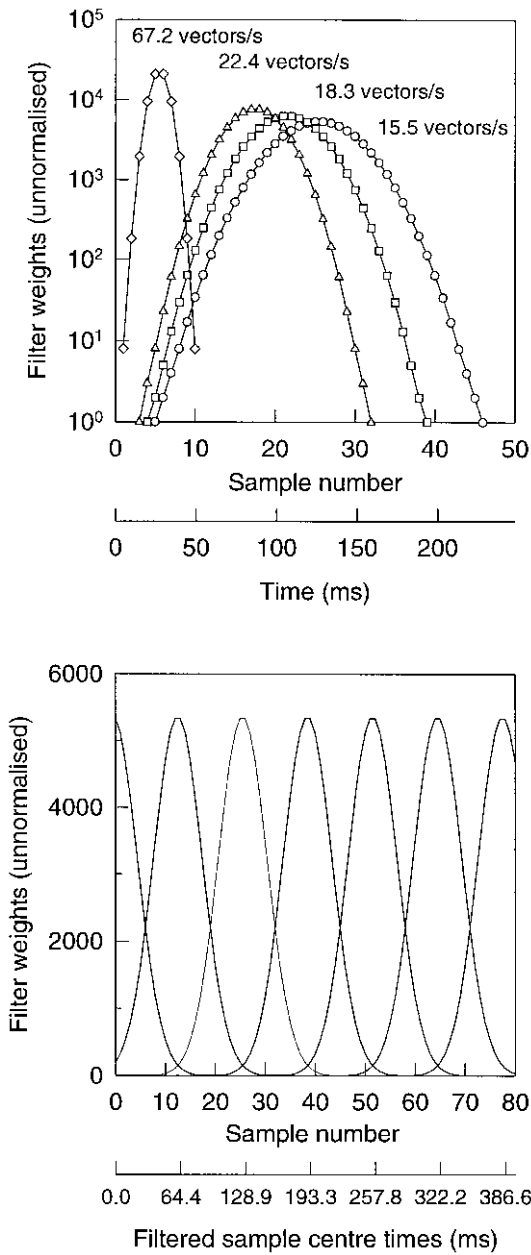


Figure 5. (a) Gaussian filter weights used in the FGM Data Processing Unit to match the internally sampled vector rate to the transmitted telemetry rate. (b) Overlap between the digitally filtered individual telemetry samples of the magnetic-field vector at the 15.5 vector  $s^{-1}$  rate.

Table IV

Spacecraft telemetry modes	FGM telemetry option	Primary sensor vector rate (vector s <sup>-1</sup> )	Secondary sensor vector rate (vector s <sup>-1</sup> )
Nominal modes 1, 2, 3	A	15.519	1.091
Burst mode 2	B	18.341	6.957
	C	22.416	3.011
Burst mode 1	D	67.249	7.759

into the operation of the MSA, to allow in-flight optimisation of its operation and to program it to recognise different classes of short-duration events.

The DPU continuously calculates the long- and short-term averages of five parameters which are used in the event detection algorithm. These are as follows:

- The ‘pseudo-variance’,  $\sigma_x = \langle |B_x - b_x| \rangle$ , representing a measure of the average scatter of the magnetic field component along the spin axis sampled at the full rate ( $b_x$ ) around the filtered and transmitted value ( $B_x$ ) of this component. The calculated pseudo-variance is transmitted regularly in the telemetry and is also used as an input to the event detection algorithm.

- The spin axis component ( $B_x$ ) of the magnetic field, corrected for offset.

- The squared magnitude of the magnetic field,  $B^2 = B_x^2 + B_y^2 + B_z^2$ , with all components corrected for offsets.

- The squared magnitude of magnetic field in the spin plane,  $B^2 = B_y^2 + B_z^2$ , corrected for offsets.

- A measure of the angular change,  $B_L^2 = (\delta B_y)^2 + (\delta B_z)^2$ , in the spin plane component of the magnetic field.

Running long- and short-term averages of the above quantities are calculated over programmable intervals. For each parameter, the difference between the long term average ( $L$ ) and the short term average ( $S$ ) is continuously compared to a programmable threshold factor ( $T$ ) multiplied by the long-term average, and the whole offset by a programmable parameter ( $O$ ). If the condition  $|L - S| > |TL| + O$  is met, a flag is set for that parameter. The instrument Event Flag is set if a programmable combination of these individual flags is detected.

Sampled vectors, at rates which can be programmed up to the full sampling rate of the instrument, are continuously written into the MSA memory. If the MSA event detection mode is enabled, the memory is frozen after a preset interval following the detection of the Event Flag in such a way that the occurrence of the event is approximately half-way through the contents of the memory. In this way, data are recorded both before and after the occurrence of the event which triggered the MSA memory. Both the triggering and readout of the MSA memory are programmable

in such a manner that its operation is optimised for the acquisition of physically significant events around the Cluster orbit.

As the data coverage around the Cluster orbit is not complete, but subject to careful planning to cover regions of greatest interest for the four-spacecraft capabilities of the mission, the overall context of the observations will not always be apparent. This can be alleviated to some extent by the magnetometer using a unique flight operations mode developed late in the pre-launch programme. In this mode, the magnetometer records spin-averaged magnetic field vectors in the MSA memory during periods without telemetry coverage and then dumps the data thus acquired when telemetry coverage is resumed. It is possible to record data in this way for up to 27 hours, thus providing the context for the intervals when all instruments acquire data. The implementation of this mode is dependent on details of the operations plans, but provides a potentially important tool for enhancing the return for the mission as a whole. The operation of the mode does not affect the use of the MSA for its original purpose of acquiring snapshots of very high resolution magnetic field data during periods of normal telemetry coverage.

The magnetometer also provides, on board, a stream of sampled vectors to other instruments through the Inter-Experiment Link (IEL), to coordinate measurement sequences and to assist on-board data reduction in real time, as a function of the direction and magnitude of the magnetic field. Vectors sampled at intervals of 64.35 ms are transmitted to the plasma ion and electron detectors (CIS and PEACE), the energetic particle detector (RAPID), to the instruments in the Wave Consortium Experiment and, at a higher clock speed, to the electron gun experiment (EDI). Additionally, the trigger signal derived in the magnetometer Microstructure Analyser, signalling the occurrence of an 'event' (as defined above), is also transmitted on the Inter-Experiment Link.

The magnetometer flight instrumentation was provided by the Goddard Space Flight Center (sensors and analogue electronics), the Institute für Weltraumforschung, Graz (Analogue-to-Digital Converters), Imperial College, London (Data Processing Unit, Spacecraft Interfaces and Power Converter), and the Technische Universität Braunschweig (Microstructure Analyser). Instrument management and integration, the spacecraft-level test programme and the Ground Support Equipment were the responsibility of Imperial College. Instrument calibration and a significant contribution to the overall magnetic cleanliness programme were the responsibility of the Technische Universität Braunschweig.

#### **4. Measurement Error Sources and Instrument Calibration**

The objectives of the magnetic field investigation on Cluster rely on the accurate measurement of vector differences between spacecraft, together with accurate knowledge of the vector differences between spacecraft locations. The correlation of the measurements also requires accurate timing. The quantitative evaluation of



the effects of errors on the four-point parameters was first given by Dunlop *et al.* (1990). This is an essential task, intended to ensure that the effect of measurement errors and uncertainties is minimised in the intrinsically complex data analysis procedures outlined in Section 2. To illustrate the necessary error analysis, we present the considerations which apply to the determination of the current density vector, using the difference approximation to curl  $\mathbf{B}$ .

The estimate of the current density vector  $\mathbf{J}$  depends on the vector differences between spacecraft locations, defined as  $\mathbf{R}_{ij} = \mathbf{R}_i - \mathbf{R}_j$ , where  $\mathbf{R}_i$  and  $\mathbf{R}_j$  are the locations of spacecraft  $i$  and  $j$ , respectively; and on the vector differences  $\mathbf{B}_{ij} = \mathbf{B}_i - \mathbf{B}_j$  between the magnetic field vectors  $\mathbf{B}_i$  and  $\mathbf{B}_j$  measured by the magnetometers on those spacecraft. The upper limit of the error in the differences in spacecraft locations can be taken as  $\mathbf{R}_{ij} = \delta \mathbf{R}$ , specified for Cluster as 10 km for each component of the difference. The total error in the differences in the magnetic field between spacecraft is  $\delta \mathbf{B}_{ij} = (\delta \mathbf{B}_i + \delta \mathbf{B}_j + \mathbf{B}_{ij}^t)$ , where  $\delta \mathbf{B}_i = \sum_k \delta \mathbf{B}_i^k$  at each spacecraft, due to frame transformation (including orthogonality) errors and offsets, and  $\delta \mathbf{B}_{ij}^t = (\delta |\mathbf{B}| / \delta t)_{ij} \delta t_{ij}$  is the error component due to inter-spacecraft timing errors.

The errors in  $\mathbf{B}_i$  and  $\mathbf{B}_j$  arise in the overall error budget through the transformations which are needed to go from the measurement frame to a geophysical frame:

$$\begin{pmatrix} B_x \\ B_y \\ B_z \end{pmatrix} = G(\rho, \psi) R(\varphi) T(\alpha\beta) \begin{pmatrix} S_1/\lambda_1 - b_1 \\ S_2/\lambda_2 - b_2 \\ S_3/\lambda_3 - b_3 \end{pmatrix},$$

where  $S_l$  is the sensor output along its  $l$  axis ( $l = 1, 2$ , or  $3$ );  $b_l$  are the offsets,  $\lambda_l$  are the sensitivities;  $\mathbf{T}$  is the transformation matrix from instrument to (spinning) spacecraft coordinates,  $\mathbf{R}$  is the despun matrix and  $\mathbf{G}$  is the transformation from the spacecraft frame into a geophysical coordinate system.

Under some assumptions the effects of the errors on the estimate of the current density can be written as

$$\frac{\delta \mathbf{J}}{|\mathbf{J}|} = S_R \frac{\delta \mathbf{R}}{\mathbf{R}_{ij}} + S_B \frac{\delta \mathbf{B}}{\mathbf{B}_{ij}},$$

where  $S_R$  and  $S_B$  are coefficients which represent the effect of the shape of the Cluster tetrahedron on the estimate. In the best case (for a regular tetrahedron)  $S_R$  and  $S_B$  are of order 1, but for deformed configurations, there is a magnifying effect, with the two coefficients of order 5 to 10. Essentially similar results were found by Robert and Roux (1993), and Robert *et al.* (1995), using a range of criteria for characterising the ‘quality’ of the tetrahedron, as it evolves around each orbit from a regular to an elongated, finally planar and even, occasionally, nearly aligned configuration (before repeating the cycle on the next orbit). In terms of

errors in the determination of the current density, typical fractional errors of order 10% are expected for spacecraft separation uncertainties of 5 to 10% for the case of the regular tetrahedron, but 50% or more when the tetrahedron is significantly distorted.

Inter-spacecraft timing errors are limited to 4 ms by specification of the Cluster mission. This introduces an uncertainty in the estimated current density which, in general, is less than that due to the inter-spacecraft distance errors.

Other four-point parameters which can be derived by the analysis tools discussed in Section 2 are similarly affected by the uncertainties in the magnetic field measurements, the spacecraft separation vectors and inter-spacecraft timing. However, the error sources enter into the analysis in a more complex manner and their effects need to be evaluated on a case-by-case basis. For instance, uncertainties associated with the determination of normal directions of discontinuity surfaces using minimum variance analysis (even in the case of single spacecraft data) are more often due to the complexity associated with phenomena near the discontinuity and the selection of the intervals used than with inherent errors in the data set.

Given that uncertainties arise not only from intrinsic instrument performance (including cross-calibration of the instruments on the four spacecraft), but from mission-associated performance and constraints (spacecraft attitude, inter-spacecraft distances, timing), error control by the magnetometer is limited to comprehensive instrument calibration, both pre-launch and in flight. Extensive instrument-level calibrations were carried out in the Magnetsrode facility of the Technische Universität, Braunschweig, with additional calibration activities at the large magnetic facility (MFSA) of the Industrieanlagen Betriebsgesellschaft (IABG) where spacecraft-level magnetic tests were also carried out.

Instrument calibration has covered the determination of the magnetic alignment of the sensors with respect to their reference (geometric) axes; offsets and sensitivity factors for all ranges; temperature dependences of these parameters; frequency and transient responses. The frequency response of the sensors is adapted to the basic sampling rate of the instrument; the results of calibration of one of the tri-axial sensors is shown in Figure 6. These pre-launch calibration parameters will serve as a first input to a continuous monitoring programme in flight. For measuring accurately the sensitivity of the magnetometers, a calibration field was switched on and off periodically, with a period of 2 s. The response of one of the sensors to a calibration field of 38 nT is shown in Figure 7(a). Given that the complete calibration sequence consists of 64 such on-off cycles of the calibration field, the response can be analysed in the frequency domain. The result of such an analysis for the frequency range 0 to 1 Hz is shown in Figure 7(b). The signal peak of 38.071 nT at 0.5 Hz shows the magnitude of the sensor response to the applied calibration field. The signal-to-noise ratio of the calibration step is of order 60 db. This result was obtained during tests at IABG, using calibrated magnetic field steps; in space a calibration voltage is applied in the magnetometer feedback loop to provide, using the same analysis techniques, an accurate check on the sensitivity of the sensors.

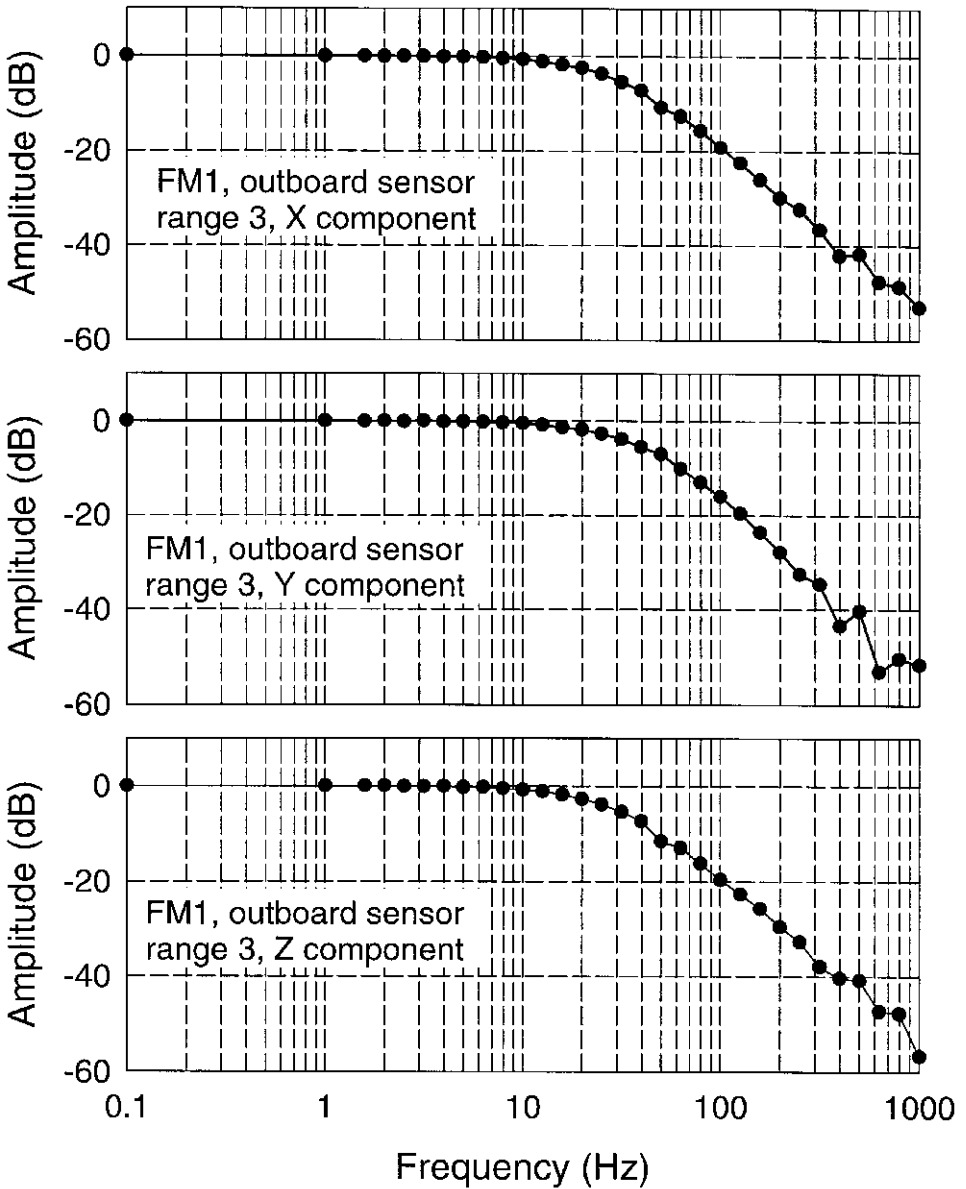


Figure 6. Analogue response of the three sensors of the one of the vector fluxgate magnetometers.

Many calibration parameters, such as alignment with respect to spacecraft axes, are susceptible to be refined in space; for some, such as offsets, continuous monitoring is essential. In-flight calibration techniques are routinely applied to magnetic-field data from single spacecraft. However, on Cluster, there is the additional opportunity to compare closely related data from four spacecraft. While such com-

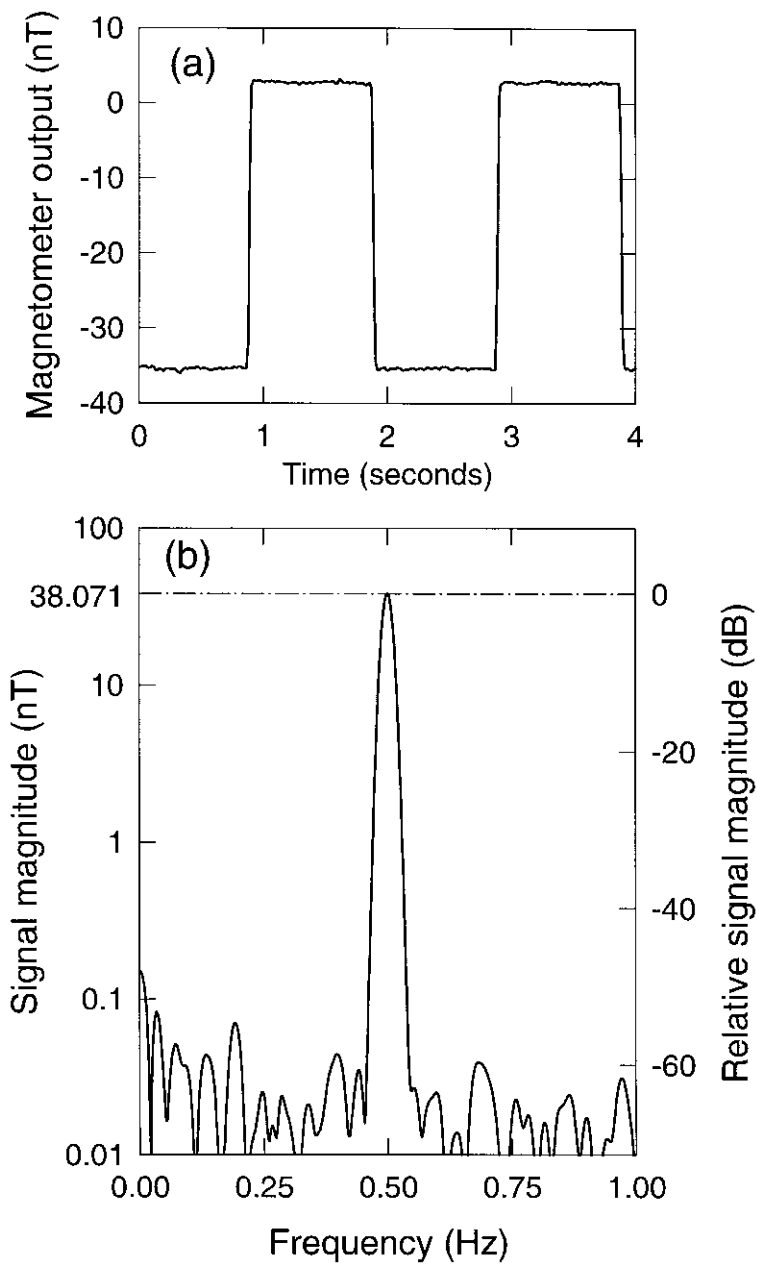


Figure 7. (a) Time domain response of one of the magnetometer sensors to the repeated application of a  $-38$  nT magnetic field. (b) Frequency domain analysis of a magnetometer sensor to a  $38$  nT magnitude,  $2$  s period,  $64$ -cycle calibration signal.

parisons are made, in the first instance, to derive differential quantities required by the basic objectives of Cluster, a systematic study of the residuals provides an opportunity directly to inter-calibrate the instruments in space.

A major potential source of uncertainties for magnetic-field measurements in space is background fields due to the spacecraft at the location of the magnetometer sensors. For the Cluster mission, as for previous ESA spacecraft with similar requirements, a comprehensive magnetic cleanliness programme was implemented, to ensure that any disturbance caused by the spacecraft is minimised. The sensors are mounted on a 5 m boom, which locates them at about 4.7 m and 6.2 m from the centre-line of the spacecraft, or at 3.2 m and 4.7 m from the surface of the spacecraft, respectively. The maximum allowable DC magnetic field at the location of the outboard magnetometer sensor is 0.25 nT; the field should not vary by more than 0.1 nT in 100 s. Strict magnetic cleanliness requirements were enforced, with all elements of the spacecraft allocated a maximum magnetic budget. All units were individually mapped and, if necessary, compensated. The magnetic signatures of all units were incorporated into a synthetic magnetic model for each spacecraft, maintained by the Technische Universität, Braunschweig. The overall magnetic signatures of all four spacecraft were measured in the MFSA-IABG facility. Three of the spacecraft were found to be outside the 0.25 nT specification, but were compensated. Results of the measured and modelled fall-off of the F3 spacecraft's magnetic field is shown in Figure 8 (taken from the report on these tests prepared by K. Mehlem); as a result of compensation, the background field at both inboard and outboard sensors is 0.12 nT, a very satisfactory value for the magnetic field investigation. The other three spacecraft have, similarly, background fields significantly better than the specification.

## 5. Operations and Data Processing Plans

The in-flight operation of the magnetometer is, in principle, simple. It basically measures a single quantity, the three components of the magnetic field vector, and transmits a time series of vectors at rates which are closely related to the operating mode of the spacecraft telemetry. The time resolution of the magnetometer in fact always exceeds by up to two orders of magnitude the time resolution of the plasma instruments, which have considerably more complex measurement tasks. As a result, the scientific operation of the mission, which includes the selection of parts of the orbit for higher time resolution, burst mode, data taking, is largely dependent on the requirements of instruments other than the magnetometer.

Science operations, in particular the planned data coverage, can be looked at from two related, but somewhat conflicting points of view. The complex interplay between the data coverage along the orbit and ground station visibility, combined with the significant, but finite on-board data storage leads to trade-offs between burst mode (high data rate) and nominal mode (standard data rate) operations.

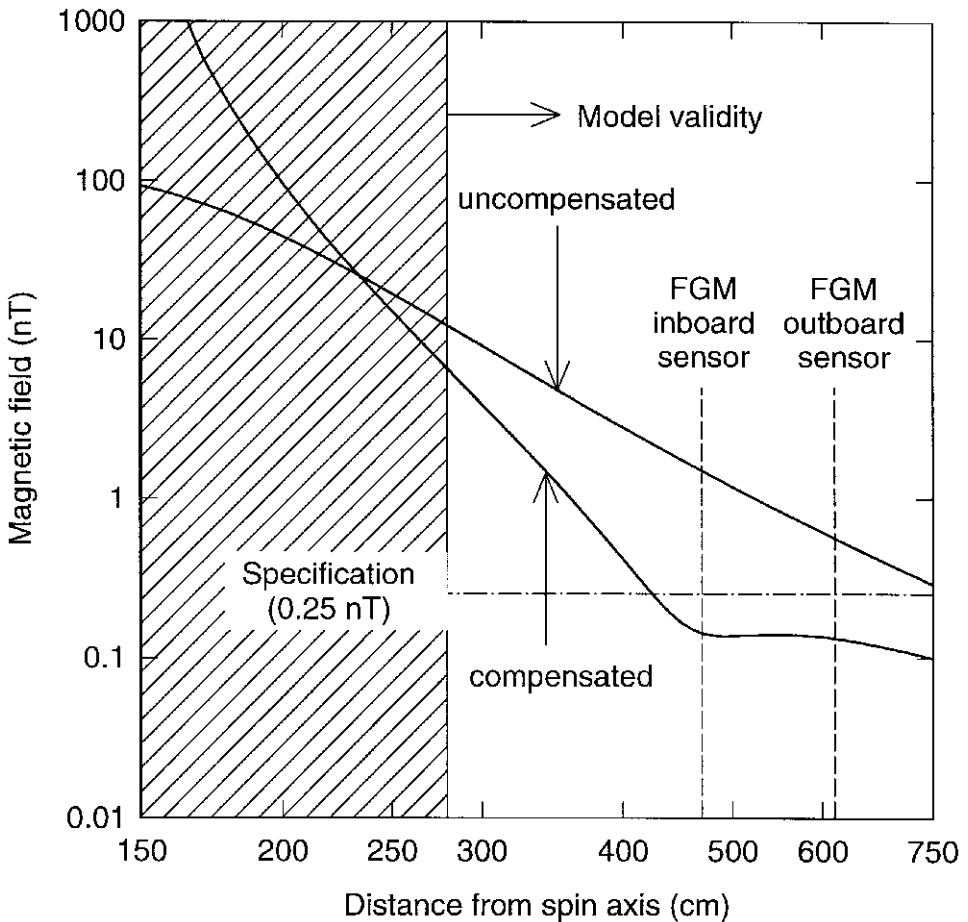


Figure 8. Measured fall-off of the spacecraft background magnetic field (compensated and uncompensated) along the axis of the magnetometer boom, showing the final low value of the magnetic disturbance caused by the spacecraft at the location of the magnetometer sensors. (The results of the modelling data are shown courtesy of K. Mehlem, ESTEC.)

While 'magnetospheric' objectives would need maximal, preferably complete coverage along the orbit, objectives associated with 'small-scale plasma processes' require operations in the high-data-rate mode, even at the expense of complete coverage. These objectives can be regarded as complementary; however, for the magnetometer (because of its inherently high sample rate) maximising the coverage along the orbit would normally be preferable.

The operation of the magnetometer will be fully coordinated through the Cluster Joint Science Operations Centre (JSOC) (Hapgood *et al.*, this issue). Inputs to science operations planning will be done through the Cluster Science Working Team and the Science Operations Working Group. Routine command generation

and monitoring of the status, health and safe operation of the instrument through access to quick-look data will be carried out from Imperial College.

Data processing development for the magnetic field investigation has been led by the Technische Universität Braunschweig, with support by Imperial College. In common with other Cluster investigations, full support has been given to the Cluster Science Data System (Schmidt and Escoubet, this issue), in particular to the UK Cluster Data Handling Facility at the Rutherford Appleton Laboratory, to generate the magnetic field Prime and Summary Parameter Data Bases, intended for use by the wider investigator community as the basis for collaborative studies. Continuous effort will be made to ensure the quality of the magnetic field Prime Parameter Data Base (PPDB) to make it suitable to serve as the basis of multi-instrument investigations. Furthermore, the need for the magnetic field data by other investigations to generate their own Prime Parameter Data will be supported by the distribution and maintenance of software (by the Hungarian Data Centre) at the national CSDS centres which will generate the magnetic-field Processing Support Data Set.

Internal to the magnetic field investigator team, software to generate full time resolution data will be used at most sites. A 1 s averaged Reference Magnetic Field data set will be generated and maintained by the team. In-flight calibration of the instrument and the generation of calibration files will be coordinated by Imperial College. An important architectural aspect of the data processing is the handling of the calibration files. Several versions of these will be generated, with a strict account maintained of their use. The routine processing of the Prime and Summary Parameter Data requires an early estimate of the calibration parameters. These needs will be covered by calibration files generated for operational use, based on an early evaluation of the calibration parameters using the results of ground calibration, passes through the quick-look data and a first pass through the complete daily data set. These operational files will be recorded but will not be re-used. A 'current best' calibration file will be generated and maintained at Imperial College which will cover the best estimates of calibration parameters covering the complete period from launch. This file will be updated as refinements are made to the calibration parameters, both at single spacecraft and four-spacecraft level.

It is expected that data gathered by the magnetometers on Cluster will provide a basic input to magnetospheric research for a duration well beyond the lifetime of the mission. Archiving plans, although at a preliminary stage, will be implemented to ensure the continued availability of the data. These plans concern specifically the Prime Parameter Data sets generated at the Cluster Data Centres, the 1 second Reference Data Set generated by the Cluster FGM team and access to high resolution data from the Cluster Raw Data Medium. For the processed data sets, archiving will consist in maintaining the data in their final calibrated state. For access to higher resolution data, archiving will consist not only in the maintenance of the raw data, but also in the maintenance of related orbit and calibration files,

the processing software, and coordinate transformation routines needed to generate calibrated data sets in geophysical coordinate systems.

## 6. Summary

- The magnetic field investigation (FGM) on Cluster will provide accurate, high time-resolution, intercalibrated four-point measurements of the magnetic-field vector in the magnetosphere and in the upstream solar wind along the Cluster orbit.
- These measurements, in conjunction with other plasma parameters measured on Cluster will enable the analysis of complex, three-dimensional processes, boundaries and their dynamics. The applicability of these techniques depends strongly on the relative size and orientation of the Cluster tetrahedron as it evolves around the orbit with respect to anisotropies and scale sizes of plasma phenomena and structures in the different regions of the magnetosphere.
- The four-point magnetic field measurements require a range of new analysis techniques which integrate classical time series analysis with modelling and simulation of the observed phenomena. The different analysis techniques rely on the detailed analysis of the error sources which arise not only from uncertainties in magnetic-field measurements but also from uncertainties in the knowledge of the Cluster geometry. Pre-flight and in-flight calibration of the magnetometers, including four-spacecraft intercalibration techniques in flight, will minimise the errors in the magnetic field measurements. The intensive magnetic-cleanliness programme has ensured that the spacecraft background will not disturb the measurements.
- The coordination of in-flight operations and the extensive data-processing programme will ensure a timely dissemination of the magnetic field data to underpin the expected cooperative data analysis programmes necessary to exploit the opportunities offered by the Cluster mission.

## Acknowledgements

We acknowledge our indebtedness to many people at the different institutions who contributed to the successful implementation of the Cluster magnetic field investigation. These have included T. Beek, C. Carr, H. Larbie, E. Serpell, B. Wingfield, T. Woodward, and S. Balogh at Imperial College; R. Kempen, H. Kùgler, M. Rahm, I. Richter, J. Warnecke at the Technische Universität Braunschweig; J. Scheifele at the Goddard Space Flight Center; O. Aydogar at the Institut für Weltraumforschung, Graz; K. Khurana at UCLA. We are grateful for the support of the Cluster Project Scientist, Dr R. Schmidt and his Deputy, Dr P. Escoubet; the support and unfailing cooperation of the ESA Cluster Project Team: J. Credland, J. Ellwood, B. Gramkow, H. Bachmann, and their colleagues; the support provided for mission analysis and operations by the ESOC Team: M. Warhaut, J. Rodriguez-Canabal, P. Ferri and their colleagues; and the professionalism of the Dornier Cluster Project Team.



Financial support for the Cluster magnetic field investigation has been provided by the Particle Physics and Astronomy Research Council in the United Kingdom, DARA in Germany, the Österreichisches Akademie der Wissenschaften in Austria and NASA in the United States.

## References

- Balogh, A., Cowley, S. W. H., Dunlop, M. W., Southwood, D. J., Thomlinson, J. G., Glassmeier, K.-H., Musmann, G., Lühr, H., Acuña, M. H., Fairfield, D. H., Slavin, J. A., Riedler, W., Schwingenschuh, K., Neubauer, F. M., Kivelson, M. G., Elphic, R. C., Primdahl, F., Roux, A., and Tsurutani, B. T.: 1993, 'The Cluster Magnetic Field Investigation: Scientific Objectives and Instrumentation', *Cluster: Mission, Payload and Supporting Activities*, ESA SP-1159, 95.
- Burgess, D.: 1989, 'Cyclic Behaviour at Quasi-Parallel Collisionless Shocks', *Geophys. Res. Letters* **16**, 345.
- Burgess, D.: 1995, 'Virtual Instruments for Space Plasmas', *Proc. Cluster Workshop on Physical Measurements and Mission Oriented Theory*, ESA SP-371, 179.
- Chapman, S. C. and Dunlop, M. W.: 1993, 'Some Consequences of the Shift Theorem for Multispacecraft Measurements', *Geophys. Res. Letters* **20**, 1033.
- Coeur-Joly, O., Robert, P., Chanteur, G., and Roux, A.: 1995, 'Simulated Daily Summaries of Cluster Four-Point Magnetic Field Measurements', *Proc. Cluster Workshop on Physical Measurements and Mission Oriented Theory*, ESA SP-371, 223.
- Cowley, S. W. H.: 1995, 'Prospects for Progress in Geotail and Substorm Studies with Cluster', *Proc. Cluster Workshop on Physical Measurements and Mission Oriented Theory*, ESA SP-371, 253.
- Credland, J. et al.: 1996, *Space Sci. Rev.*, this issue.
- Dunlop, M. W.: 1990, 'Review of the Cluster Orbit and Separation Strategy: Consequences for Measurements', *Proc. Int. Workshop on Space Plasma Physics Investigations by Cluster and Regatta*, ESA SP-306, 17.
- Dunlop, M. W. and Balogh, A.: 1993, 'On the Analysis and Interpretation of Four-Spacecraft Magnetic Fields Measurements in Terms of Small Scale Plasma Processes', *Spatio-Temporal Analysis for Resolving Plasma Turbulence*, ESA WPP-047, 223.
- Dunlop, M. W., Southwood, D. J., Glassmeier, K.-H., and Neubauer, F. M.: 1988, 'Analysis of Multi-Point Magnetometer Data', *Adv. Space Res.* **8** (9), 273.
- Dunlop, M. W., Balogh, A., Southwood, D. J., Elphic, R. C., Glassmeier, K.-H., and Neubauer, F. M.: 1990, 'Configurational Sensitivity of Multipoint Magnetic Field Measurements', *Proc. Int. Workshop on Space Plasma Physics Investigations by Cluster and Regatta*, ESA SP-306, 23.
- Dunlop, M. W., Southwood, D. J., and Balogh, A.: 1993, 'The Cluster Configuration and the Directional Dependence of Coherence Lengths in the Magnetosheath', *Spatio-Temporal Analysis for Resolving Plasma Turbulence*, ESA WPP-047, 295.
- Dunlop, M. W., Woodward, T. I., Motschmann, U., Southwood, D. J., and Balogh, A.: 1996, 'Analysis of Non-Planar Structures with Multipoint Measurements', *Adv. Space Res.* **18** (8), 309.
- Dunlop, M. W., Woodward, T. I., and Farrugia, C. J.: 1995a, 'Minimum Variance Analysis: Cluster Themes', *Proc. Cluster Workshop on Data Analysis Tools*, ESA SP-371, 33.
- Dunlop, M. W., Woodward, T. I., Motschmann, U., Glassmeier, K.-H., Southwood, D. J., and Balogh, A.: 1995b, 'Analysis of Non-Planar Structures with Multi-Point Techniques: a Roadmap for Cluster?', *Proc. Cluster Workshop on Physical Measurements and Mission Oriented Theory*, ESA SP-371, 267.
- Elphic, R. C.: 1988, 'Multipoint Observations of the Magnetopause: Results from ISEE and AMPTE', *Adv. Space Res.* **8** (9), 223.
- Escoubet, P. and Schmidt, R.: 1996, 'Cluster – Science and Mission Overview', *Space Sci. Rev.*, this issue.
- Ferri, P. and Warhaut, M.: 1996, 'Cluster Mission Operations', *Space Sci. Rev.*, this issue.

- Giacalone, J., Schwartz, S. J., and Burgess, D.: 1994, 'Artificial Spacecraft in Hybrid Simulations of the Quasi-Parallel Earth's Bow Shock: Analysis of Time Series Versus Spatial Profiles and a Separation Strategy for Cluster', *Ann. Geophys.* **12**, 591.
- Glassmeier, K.-H., Motschmann, U., and Stein, R. von: 1995, 'Mode Recognition of MHD Wave Fields at Incomplete Dispersion Measurements', *Ann. Geophys.* **13**, 76.
- Hapgood, M. A., Trimbylow, T. G., Sutcliffe, D. C., Chaizy, P. A., Ferran, P. S., Hill, P. M., and Tiratay, X. T.: 1996, 'The Joint Operations Centre', *Space Sci. Rev.*, this issue.
- Motschmann, U. and Glassmeier, K.-H.: 1995, 'Mode Recognition of MHD Wave Fields', *Proc. Cluster Workshop on Data Analysis Tools*, ESA SP-371, 103.
- Motschmann, U., Woodward, T. O., Glassmeier, K.-H., and Dunlop, M. W.: 1995a, 'Array Signal Processing Techniques', *Proc. Cluster Workshop on Data Analysis Tools*, ESA SP-371, 79.
- Motschmann, U., Woodward, T. I., Glassmeier, K.-H., and Southwood, D. J.: 1995b, 'Wavelength and Direction Filtering by Magnetic Measurements of Satellite Arrays: Generalised Minimum Variance Analysis', *J. Geophys. Res.*, submitted.
- Neubauer, F. M. and Glassmeier, K.-H.: 1990, 'Use of an Array of Satellites as Wave Telescope', *J. Geophys. Res.* **95**, 19 115.
- Neubauer, F. M., Glassmeier, K.-H., Walter, R., and Dunlop, M. W.: 1990, 'Cluster as a Wave Telescope', *Proc. Int. Workshop on Space Plasma Physics Investigations by Cluster and Regatta*, ESA SP-306, 51.
- Opgenoorth, H. J. et al.: 1996, 'Opportunities for Magnetospheric Research with Coordinated Cluster and Ground-Based Measurements', *Space Sci. Rev.*, this issue.
- Paschmann, G.: 1995, 'Magnetopause, Cusp and Dayside Boundary Layer: Experimental Point of View', *Proc. Cluster Workshop on Physical Measurements and Mission Oriented Theory*, ESA SP-371, 149.
- Pinçon, J. L.: 1995, 'Cluster and the  $k$ -filtering', *Proc. Cluster Workshop on Physical Measurements and Mission Oriented Theory*, ESA SP-371, 87.
- Pinçon, J. L. and Lefeuvre, F.: 1991, 'Local Characterization of Homogeneous Turbulence in a Space Plasma from Simultaneous Measurement of Field Components at Several Points in Space', *J. Geophys. Res.* **96**, 1789.
- Robert, P. and Roux, A.: 1990, 'Accuracy of the Estimate of  $J$  via Multipoint Measurements', *Proc. Int. Workshop on Space Plasma Physics Investigations by Cluster and Regatta*, ESA SP-306, 23.
- Robert, P. and Roux, A.: 1993, 'Dependence of the Shape of the Tetrahedron on the Accuracy of the Estimate of the Current Density', *Spatio-Temporal Analysis for Resolving Plasma Turbulence*, ESA WPP-047, 289.
- Robert, P., Roux, A., and Coeur-Joly, O.: 1995, 'Validity of the Estimate of the Current Density Along the Cluster Orbit with Simulated Magnetic Field Data', *Proc. Cluster Workshop on Physical Measurements and Mission Oriented Theory*, ESA SP-371, 229.
- Roux, A. and Sauvaud, J. A.: 1995, 'Splinter Session on Magnetotail and Substorms', *Proc. Cluster Workshop on Physical Measurements and Mission Oriented Theory*, ESA SP-371, 205.
- Russell, C. T.: 1988, Multipoint measurements of upstream waves, *Adv. Space Res.* **8** (9), 147.
- Schmidt, R. and Escoubet, C. P.: 1996, 'The Cluster Science Data System (CSDS) – a New Approach to the Distribution of Scientific Data', *Space Sci. Rev.*, this issue.
- Scholer, M.: 1995, 'Magnetopause, Cusp and Dayside Boundary Layer: Theoretical Point of View', *Proc. Cluster Workshop on Physical Measurements and Mission Oriented Theory*, ESA SP-371, 153.
- Scholer, M. and Burgess, D.: 1992, 'The Role of Upstream Waves in Supercritical Quasi-Parallel Shock Re-Formation', *J. Geophys. Res.* **97**, 8319.
- Scholer, M., Fujimoto, M., and Kucharek, H.: 1993, 'Two-Dimensional Simulations of Supercritical, Quasi-Parallel Shocks: Upstream Waves, Downstream Waves and Shock Re-Formation', *J. Geophys. Res.* **98**, 18 971.
- Sonnerup, B. U. O. and Cahill, L. J.: 1967, 'Magnetopause Structure and Attitude from Explorer 12 Observations', *J. Geophys. Res.* **72**, 171.
- Southwood, D. J.: 1990, 'Multispacecraft Measurements at Varying Scalelengths – the Cluster/Regatta Opportunity', *Proc. Int. Workshop on Space Plasma Physics Investigations by Cluster and Regatta*, ESA SP-306, 1.

- Thomsen, M. F.: 1988, 'Multi-Spacecraft Observations of Collisionless Shocks', *Adv. Space Res.* **8** (9), 157.
- Tsyganenko, N. A.: 1987, 'Global Quantitative Models of the Geomagnetic Field in the Cislunar Magnetosphere for Different Disturbance Levels', *Planetary Space Sci.* **35**, 1347.
- von Stein, R., Glassmeier, K.-H., and Motschmann, U.: 1993, 'Cluster as a Wave Telescope and Mode Filter', *Spatio-Temporal Analysis for Resolving Plasma Turbulence*, ESA WPP-047, 211.
- Watkins, N. W., Chapman, S. C., and Dunlop, M. W.: 1995, 'Fourier Techniques in Space Plasma Measurements', *Proc. Cluster Workshop on Physical Measurements and Mission Oriented Theory*, ESA SP-371, 235.